Analysis of L-Probe Fed-Patch Microstrip Antennas in a Multilayered Spherical Media

TaoYu, Chengyou Yin
National Key Laboratory of Pulsed Power Laser Technology of Electronic Engineering Institute,
Address: 460 Huangshan Rd. Hefei, Anhui, China, 230037

***Abstract*-In this paper, the L-probe fed-patch microstrip antennas in a multilayered spherical media are analyzed based on the method of moments (MoM). Firstly, the structures of microstrip antennas in three-layered spherical media fed by L-probe are established as similar as the plane case. Then, the method of moments is employed to solve the mixed potential integral equation (MPIE). Numerical results for the input impedance, radiation patterns are showed good agreement with ones come from commercial software FEKO. Finally, the effects of all kind of geometric parameters on the characteristics of antenna are investigated for the next design purpose.**

I. INTRODUCTION

As we know, the microstrip antenna is a kind of resonance antenna and the narrow bandwidth is the major weakness. Much effort has been done to widen the bandwidth of microstrip in plane case in past decades, including impedance matching technology [1] and using thick substrates [2]. The feeding approach employing L-probe is an effective method to ameliorate bandwidth, which is especially convenient for the coplanar case. The microstrip antenna with an L-probe in planar case has been studied in [3]-[5]. A modified L-probe fed microstrip antenna has been presented in [6].

Compared with in planar case, only a few literatures relate to the microstrip antenna with L-probe in coplanar case [7]. The conformal microstrip antennas have a major advantage that they have a wider angular radiation pattern than the planer counterparts. It is worthwhile to research the characteristics of the antennas with L-probe in conformal case.

In this paper, the L-probe patch antenna in a multilayered spherical media is studied by employing the method of moments (MoM). The structure of antenna is obtained with the aid of commercial software FEKO, which is divided into a mesh of triangular patches. The surface current density can be calculated by solving the mixed potential integral equation (MPIE) based on the Rao-Wilton-Glisson (RWG) basis function. Characteristics including input impedance, radiation pattern are presented, which agree well with those from FEKO. Finally, extensive numerical results of antenna parametric study are showed in order to provide some design information.

II. THEORY

A. Structure of Antenna

The structure of antenna has three layers as shown in Fig.1. The innermost layer is a perfectly conducting spherical core, which can be modeled assuming the permeability tends to zero and permittivity tends to infinity [8]. The outermost layer assumed to be free space. The rectangular patch locates at interface of medium layer and free space and the conformal L-probe positions at the medium layer. Detailed parameters are shown in Fig.1. In this paper, nonmagnetic materials have been considered, that is $\mu_r = 1$.

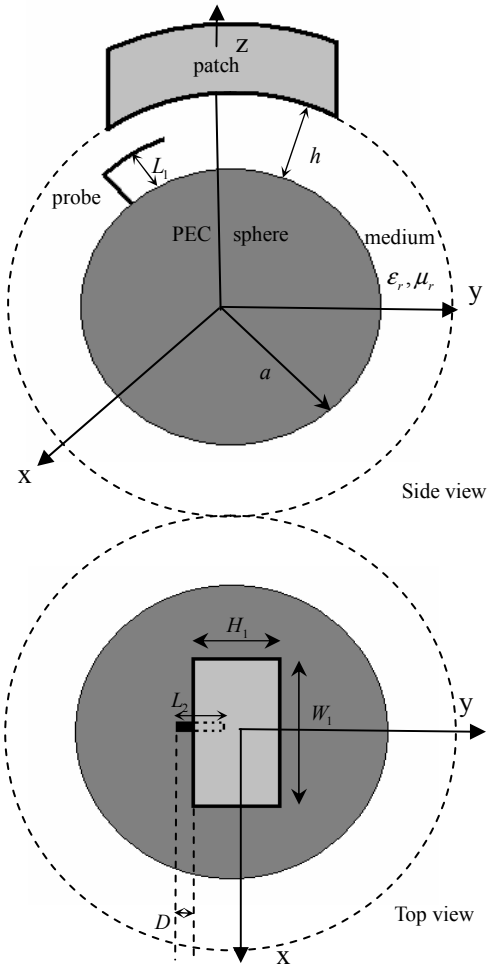

Figure 1. Structure of antenna with L-probe

B. Mixed potential integral equation

In this paper, MoM is employed to solve the problem because of its accuracy and efficient. In order to make analysis process simplification, the L-probe can be treated as an L-trip [9], which is connected to the PEC spherical core. A delta gap voltage source has been placed at the base of the feeding trip. The tangential electric field can be achieved employing the mixed potential integral equation:

$$\boldsymbol{E}^i|_t = -j\omega\mu_f \iint_{s'} \bar{\boldsymbol{G}}_A \bullet \boldsymbol{J}_s(r')ds' - \nabla \iint_{s'} \nabla' G_\varphi \bullet \boldsymbol{J}_s(r')ds'|_t \quad (1)$$

where μ_f represents the permeability of the layer of field point. s' is the surface area of the antenna conducting body except the ground sphere as shown in Fig.2, and $\boldsymbol{J}_s(r')$ is the current density of the surface area. The contribution of the ground sphere has been incorporated in the Green's functions including magnetic vector potential Green's function $\bar{\boldsymbol{G}}_A$ and electric scalar potential Green's function G_φ.

Solving the dyadic Green function in spherically multi-layered media is indispensable in order to make the analysis results accurate. A general expression of the dyadic Green's function for the electromagnetic fields in an arbitrary multi-layered medium has been achieved in [10]. Further development of Green's function has been proposed in [8], where the electric field Green's function was transformed to the mixed potential Green's function. Take G_φ component for example:

$$G_\varphi = -\frac{\omega\mu_f}{4\pi k_f}\sum_{n=1}^{\infty}\frac{2n+1}{n(n+1)}\times \begin{pmatrix} \partial h_n^{(2)}(k_s r)\left[A_n^{TM}\partial h_n^{(2)}(k_f r') + B_n^{TM}\partial j_n(k_f r')\right] \\ +\partial j_n(k_s r)\left[C_n^{TM}\partial h_n^{(2)}(k_f r') + D_n^{TM}\partial j_n(k_f r')\right] \end{pmatrix} \bullet P_n(\cos\gamma) \quad (2)$$

meaning of the denotations can be found in [8]. From the expressions, we can see that the above expression is an infinite summation of spherical harmonics. In order to accelerate the convergence of the infinite series, asymptotic extraction approach has been adopted in [11]-[12].

The surface area of the antenna conducting body has been divided into a mesh of triangular patches as shown in Fig.2, and the RWG triangular function is the most appropriate basis function [13]. Then, we expand the current $\boldsymbol{J}_s(r')$ via a sum of weighted basis functions:

$$\boldsymbol{J}_s(r') = \sum_{n=1}^{N} a_n \boldsymbol{f}_n(r') \quad (3)$$

and the method of Galerkin has been adopted in this paper. Every element of the impedance matrix can be obtained by the expression below:

$$Z_{mn} = \iint_s \iint_{s'} \begin{bmatrix} j\omega\mu_f \boldsymbol{f}_m(\boldsymbol{r}) \bullet \bar{\boldsymbol{G}}_A \bullet \boldsymbol{f}_n(\boldsymbol{r}') + \\ (\nabla \bullet \boldsymbol{f}_m(\boldsymbol{r}))G_\varphi(\nabla' \bullet \boldsymbol{f}_n(\boldsymbol{r}')) \end{bmatrix} ds ds' \quad (4)$$

where m and n refer to the test and expansion function.

The electric field can be expressed as:

$$\boldsymbol{E}_n = \iint_{s'} j\omega\mu_f \bar{\boldsymbol{G}}_A \bullet \boldsymbol{f}_n(r') + \nabla(\nabla' G_\varphi \bullet \boldsymbol{f}_n(r'))ds' \quad (5)$$

A problem that needs special attention is the connection of the feeding trip to the perfectly conducting sphere. The delta gap voltage source has been placed at the connection, and more detailed analysis can be found in [14].

C. *Numerical results*

An L-probe fed-patch microstrip antenna in multilayered media has been calculated, which has the following parameters: $W_1 = 30\,mm$, $H_1 = 25\,mm$, $a = 50mm$, $L_1 = 4.95mm$, $L_2 = 9.5mm$ and $D = 2mm$. The spherical substrate has a relative permittivity of $\varepsilon_r = 1.01$ and a thickness of $h = 6.6\,mm$. The L-probe has been modeled as a strip of 2 mm width. The numerical results as shown in Fig. 3-6 are verified by comparison with the results from commercial software FEKO.

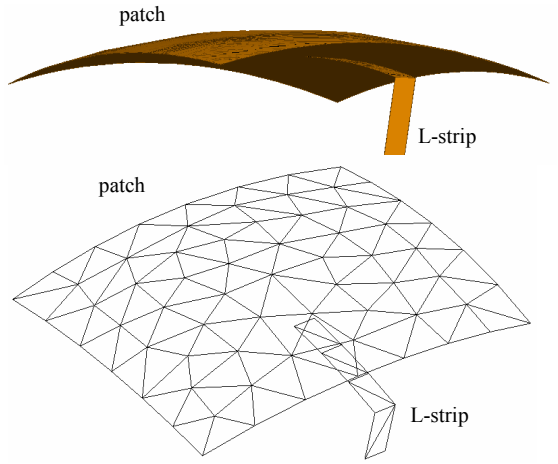

Figure 2. Surface area of antenna and mesh of the antenna

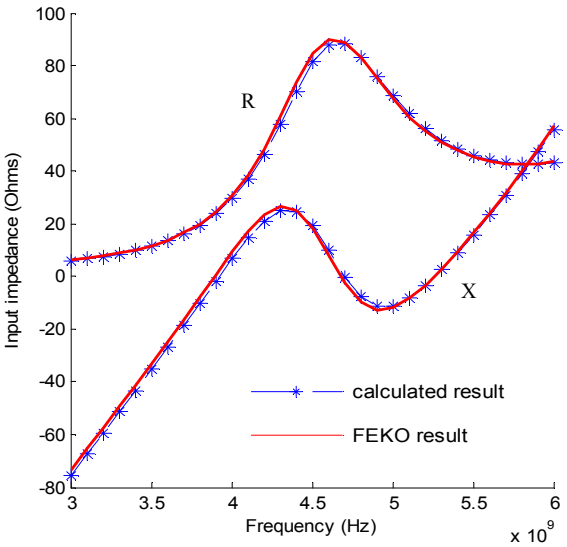

Figure 3. Input impedance versus frequency

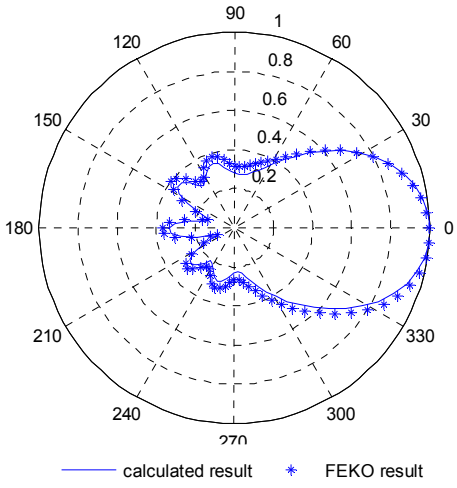

Figure 4. Far-field radiation pattern at 4.5 GHz ($\varphi = 90^\circ$)

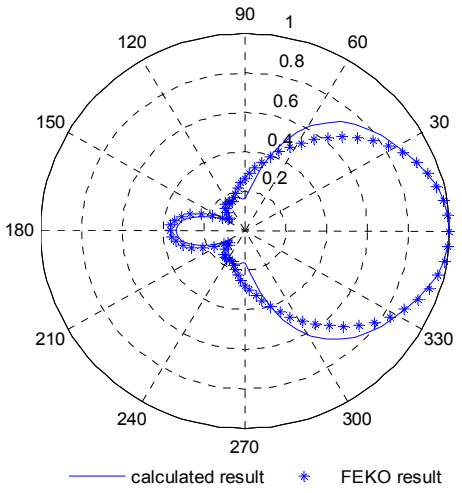

Figure 5. Far-field radiation pattern at 4.5 GHz

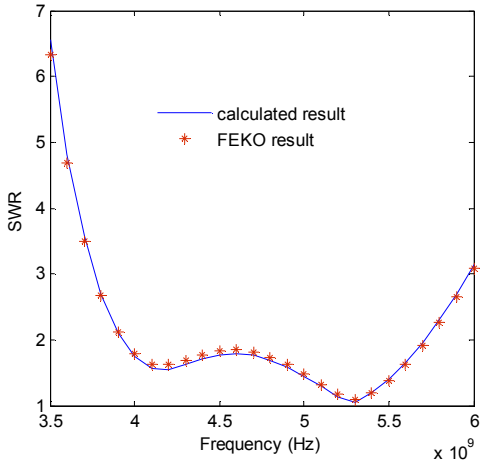

Figure 6. SWR of the antenna

From above figures, we can see that the calculated result of input impedance show good well agreement with the one from FEKO, and a small error is observed between far-field radiation pattern calculated and FEKO. The main reason is that the meshes of the two antennas are different and only surface area of antenna is meshed in this paper, while the whole antenna is meshed in FEKO. The error can be ignored that is acceptable in engineering designs. Fig. 6 shows the SWR of the antenna calculated by this paper and FEKO. From the figure, we can see the antenna attains an about 1.7 GHz impedance bandwidth (from 3.95 GHz to 5.65 GHz, $SWR \le 2$), which is similar to that in planar case [2], and wider than that of antenna fed by straight probe.

III. PARAMETRIC STUDY

In this section, we will investigate the variation of the antenna characteristics with the antenna parameters including W_1, H_1, L_1, L_2 and D. Because of the limited paper space, only the input impedances are shown, and the far-field radiation pattern and SWR of the antennas are not shown in this paper.

The variation of the input impedance with the length of patch W_1 is illustrated in Fig. 7. From the figure, we can see that input resistance decreases with increasing W_1 and the input reactance decreases before the resonant frequency and increases after the resonant frequency with increasing W_1.

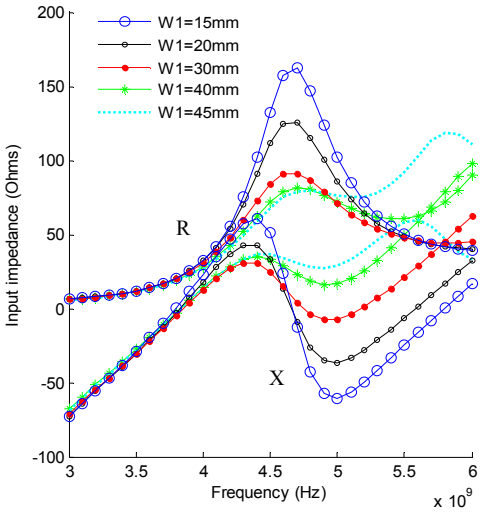

Figure 7. Input impedance versus frequency for different W_1 ($H_1 = 25mm$, $L_1 = 4.95mm$, $L_2 = 10mm$, $h = 6.6mm$ and $D = 2mm$)

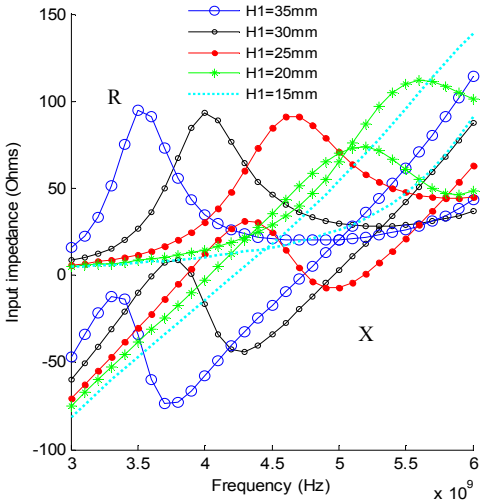

Figure 8. Input impedance versus frequency for different H_1 ($W_1 = 30mm$, $L_1 = 4.95mm$, $L_2 = 10mm$, $h = 6.6mm$ and $D = 2mm$)

The variation of the input impedance with the patch width H_1 is shown in Fig. 8. It can be observed that H_1 determined the resonant frequency of the antenna. The resonant frequency becomes high with decreasing H_1.

Fig. 9 and Fig. 10 show the variation of the input impedance with the vertical length L_1 and the horizontal length L_2 of the L-strip, respectively. We can see from the figures that both the input resistance and reactance increase with L_1, L_2. At the resonant frequency, the input resistance increases clearly with increasing L_1, and the reactance increases clearly with increasing L_2.

The effect of changing the position D of the L-strip from the patch is studied as shown in Fig. 11. $D > 0$ denotes that the L-strip is partly covered by the patch, and $D < 0$ denotes the strip is covered by the patch in whole. We can see that both the resistance and reactance change slightly when $D \ge 0$, and decrease clearly when $D < 0$.

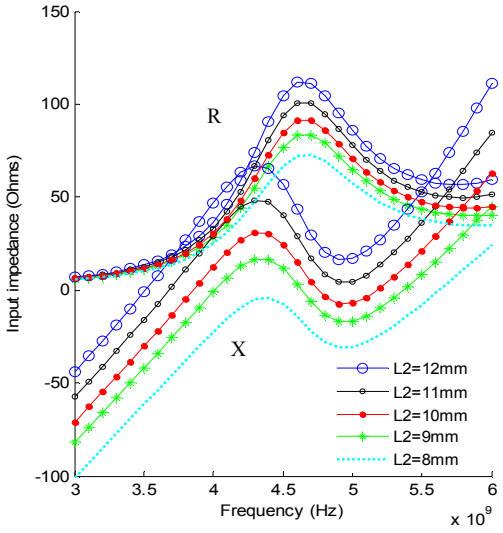

Figure 10. Input impedance versus frequency for different L_2

($W_1 = 30mm$, $H_1 = 25mm$, $L_1 = 4.95mm$, $h = 6.6mm$ and $D = 2mm$)

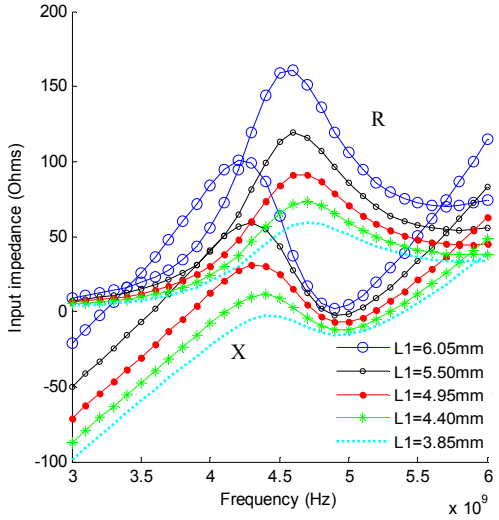

Figure 9. Input impedance versus frequency for different L_1

($W_1 = 30mm$, $H_1 = 25mm$, $L_2 = 10mm$, $h = 6.6mm$ and $D = 2mm$)

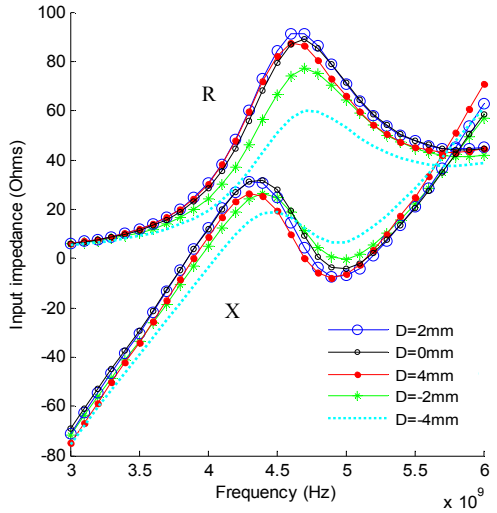

Figure 11. Input impedance versus frequency for different D

($W_1 = 30mm$, $H_1 = 25mm$, $L_1 = 4.95mm$, $L_2 = 10mm$ and $h = 6.6mm$)

IV. Conclusion

In this paper, the L-probe patch antenna in a multilayered spherical media is studied by employing the method of moments. The RWG function is regarded as bases function and test function for solving the mixed potential integral equation. Numerical results for input impedance, far-field radiation pattern are presented and verified by comparison with the results from commercial software FEKO. The effects of various parameters on the characteristics of the L-strip patch microstrip antenna have been investigated. From results obtained, we can see that the input impedance is sensitive to W_1, L_1 and L_2. The resonant frequency is determined by the parameter H_1. The effects of various parameters here are similar to that in planar case.

References

[1] H. F. Pues and A. R. Van de Capelle, "An impedance matching technique for increasing the bandwidth of microstrip antennas," *IEEE Trans. Antennas Propagat.*, vol. 37, pp.1345-1354, Nov. 1989.

[2] E. Chang, S. A. Long, and W. F. Richards, "Experimental investigation of electrically thick rectangular microstrip antennas," IEEE Trans. Antennas Propagat., vol. AP-43, pp. 767-772, 1986.

[3] Y. X. Guo, C. L. Mark and K. M. Luk, "Analysis and design of L-probe proximity fed-patch antennas," *IEEE Trans. Antennas Propagat.*, vol. 49, pp. 145-149, Feb. 2001.

[4] C. L. Mark, K. M. Luk and K. F. Lee, "Experimental Study of a micro-strip patch antenna with an L-shaped probe," *IEEE Trans. Antennas Propagat.,* vol. 48, pp. 777-783, May 2000.

[5] J. Park, H. Na and S. Baik, "Design of a modified L-probe fed micro-strip patch antenna," *IEEE Antennas Wire. Propagat. Let.,* vol. 3, pp. 117-119, 2004.

[6] H. Wong, K. L. Lau and K. M. Luk, "Design of dual-polarized L-probe patch antenna arrays with high isolation," *IEEE Trans. Antennas Propagat.*, vol. 52, pp. 45-52, Jan. 2004.

[7] X. Y. Cao, P. Li and K. M. Luk, "Efficient analysis of L-probe coupled patch antenna arrays mounted on a finite conducting cylinder," *Micro. Opt. Techno. Let.,* vol. 41, pp. 403-407, 2004.

[8] S. K. Khamas, "Electromagnetic radiation by antennas of arbitrary shape in a layered spherical media," *IEEE Trans. Antennas Propagat.*, vol. 57, pp. 3827-3834, Dec. 2009.

[9] C. Butler, "The equivalent radius of a narrow conducting trip," *IEEE Trans. Antennas Propagat.*, vol. AP-30, pp. 755-758, Jul. 1982.

[10] L. W. Li, P. S. Kooi, M. S. Leong and T. S. Yeo, " Electromagnetic dyadic Green's function in spherically multilayered media," *IEEE Trans. Micro. Theory and Techniques,* vol. 42, pp. 2302-2310, Dec. 1994.

[11] S. K. Khamas, "Asymptotic extraction approach for antennas in a multi-layered spherical media," *IEEE Trans. Antennas Propagat.*, vol. 58, pp. 1003-1008, Mar. 2010.

[12] S. K. Khamas, "A Generalized asymptotic extraction solution for antennas in multilayered spherical media," *IEEE Trans. Antennas Propagat.*, vol. 58, pp. 3743-3747, Nov. 2010.

[13] S. M. Rao, D. R. Wilton and A. W. Glisson, "Electromagnetic scattering by surfaces of arbitrary shape," *IEEE Trans. Antennas Propagat.*, vol. AP-30, pp. 409-418, May 1982.

[14] T. Yu, C. Y. Yin and H. Y. Liu, "Full-wave analysis for antennas in the presence of the metal sphere based on RWG-MoM," *Journal of Microwaves (Chinese)*, vol. 28, pp. 23-28, Feb. 2012.